

Interaction of molecular motors can enhance their efficiency

FRANTIŠEK SLANINA¹

¹ *Institute of Physics, Academy of Sciences of the Czech Republic, Na Slovance 2, CZ-18221 Praha, Czech Republic*

PACS 05.40.-a – Fluctuation phenomena, random processes, noise, and Brownian motion

PACS 87.16.Nn – Motor proteins (myosin, kinesin dynein)

PACS 07.10.Cm – Micromechanical devices and systems

Abstract. - Particles moving in oscillating potential with broken mirror symmetry are considered. We calculate their energetic efficiency, when acting as molecular motors carrying a load against external force. It is shown that interaction between particles enhances the efficiency in wide range of parameters. Possible consequences for artificial molecular motors are discussed.

Molecular motors [1–8] are fascinating objects of study for nanoscience, be it inspired by genuine biological questions of transport within the cell or by the perspective of their artificial manufacturing en masse [9–12].

Indeed, in a living cell, many macromolecules move with the help of some machine, usually made of various proteins and powered by ATP hydrolysis [13]. Not only muscle contraction, bacterial flagellum movement and changes in the shapes of amoebae are directly powered by the action of molecular motors, but many more processes [2, 14, 15] rely on motor proteins too.

A very challenging problem is the reported high efficiency of energy conversion in biological motors [8]. On the model level, the energetic efficiency was thoroughly studied [16–21]. It turns out that it is very low in classical setups of Brownian motors, which is either the flashing or the rocking ratchet [5, 18]. On the other hand, a scheme named “reversible ratchet” [20, 22, 23] was introduced, which was shown to be much more efficient, and high efficiency was also characteristic of the two-state model [24].

One of the astonishing and not yet fully understood aspects of molecular motors is their collective behaviour. Motor proteins carrying a load very often act in small but coordinated groups [8]. In gene transcription and translation large number of motor proteins move along the same track [14]. Strong interactions of hard-core type between individual motors occur in such situations.

The collective movement of coupled Brownian motors was studied [25, 26] as well as cooperative effects of hard-rod molecules in thermal ratchets [27–29]. In these studies, very complex dependence of the current on the size of the molecules was established. Collective effects were found

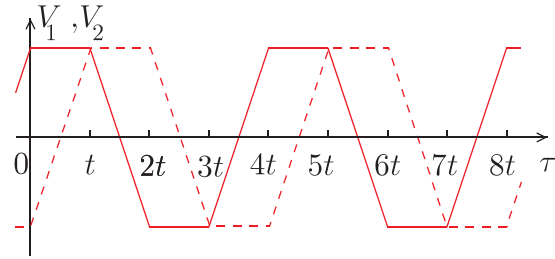


Fig. 1: Graph of the time dependence of the potential in which the particles move. Full line: $V_1(\tau)$, dashed line: $V_2(\tau)$. The potential at the third site, V_0 , is time independent.

to induce non-zero current even in mirror symmetric potential due to dynamical symmetry breaking [24]. Recent studies show that cooperative movement of several motors is the generic feature of cargo transport within the cell [7, 30].

Slightly different perspective was adopted in the studies of interactions in the transport of kinesin [31], ribosomes [32], and RNA polymerase [33]. Here, no details on the ratchet mechanism are assumed and the processes at work are idealised in the set of transition rates between the states representing spatial positions and internal conformations of the motor proteins.

In our work we assume that the motor particles move in explicit, although crudely simplified, time-dependent potential of the type used in “reversible ratchet” models [20, 22]. We shall aim at clarification of the role of interactions on the energetic efficiency of the motors.

Our model consists of N particles occupying integer positions on the segment of length L , with periodic boundary

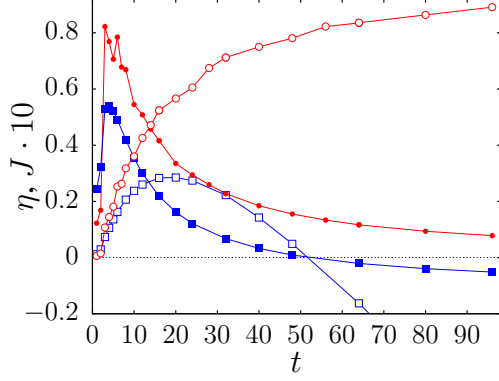


Fig. 2: Efficiency (empty symbols) and current (full symbols) as a function of the quarter-period. The temperature is $T = 0$ (\circ , \bullet) and $T = 40$ (\square , \blacksquare). Other parameters are $L = 1200$, $N = 1200$, $g = 1/9$, and $F = 0.2$.

conditions. Let us denote $x_i(\tau)$ the position of i -th particle at time $\tau = 1, 2, 3, \dots$. The configuration of other particles as seen by the j -th particle is described by the function $n_j(x, \tau) = \sum_{i, i \neq j} \delta(x - x_i(\tau))$, where $\delta(x) = 1$ if $x = 0$ and zero otherwise.

The j -th particle moves in the potential

$$U_j(x, \tau) = V(x, \tau) + xF + gn_j(x, \tau) \quad (1)$$

composed of three parts. The first term is spatially and temporally periodic external driving potential $V(x, \tau) = V_{x \bmod 3}(\tau)$. We chose the smallest non-trivial spatial period 3 for convenience, although larger periods may offer further interesting effects. The second part comes from the uniform and static external force F against which a useful work is done. Third, there is repulsive on-site interaction between particles, with strength $g \geq 0$.

The time-dependent potential evolves in a four-stroke cycle sketched in Fig. 1. The duration of every stroke is the quarter-period t . The potential has three independent values, $V_a(\tau)$, $a = 0, 1, 2$, with $V_a(\tau) = V_a(\tau - 4t)$. We fix $V_0(\tau) = 0$ and the other two evolve in a piecewise linear pattern

$$V_1(\tau) = -V_1(\tau + 2t) = \begin{cases} V & \text{for } 0 < \tau < t \\ V + 2(1 - \tau/t)V & \text{for } t < \tau < 2t \end{cases} \quad (2)$$

with a phase shift $V_1(\tau) = V_2(\tau + t)$. Note, however, that the time τ is discrete, so the potential actually undergoes finite jumps, rather than smooth change. In the following we shall always set the amplitude to $V = 1$. The potential can be understood as a travelling wave. A simplistic picture is that the particle is captured within one of the minima and is drifted by the moving wave. However, random diffusion, which is effective even at zero temperature, makes the things complex.

The particles can move to nearest neighbour sites with probabilities determined by the difference in potential (1).

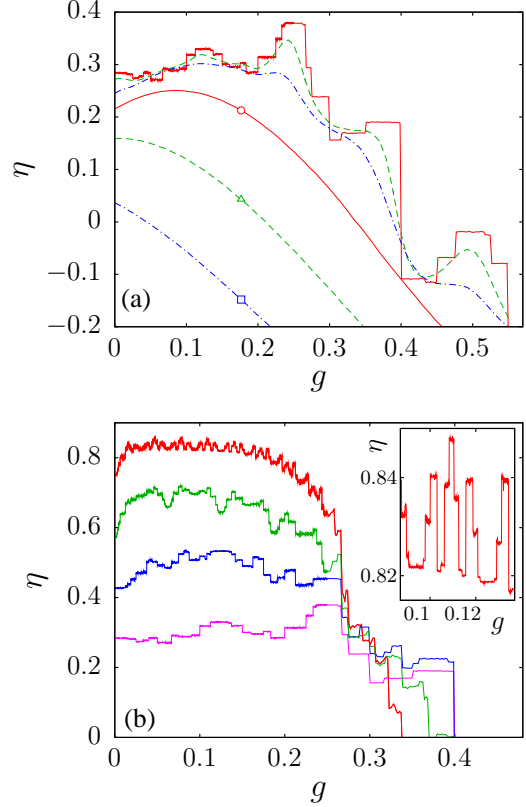


Fig. 3: Dependence of the efficiency on interaction strength, for $L = 1200$, $N = 1200$, and $F = 0.2$. Panel (a): $t = 8$, temperatures $T = 0$ (solid line), $T = 5$ (dashed line), $T = 10$ (dash-dotted line), $T = 30$ (solid line marked by \circ), $T = 60$ (dashed line marked by \triangle), and $T = 100$ (dash-dotted line marked by \square). Panel (b): $T = 0$ and quarter-periods (from top to bottom) $t = 64$, $t = 32$, $t = 16$, $t = 8$, and $t = 4$. The “noise” in the curve for $t = 64$ is in fact a complicated deterministic dependence, as can be seen in the inset, where enlarged particular of the curve is shown.

Thus, if $|x - y| = 1$, the j -th particle hops from site x to y with probability

$$W_{j,x \rightarrow y} = \frac{1}{2} \left(1 + e^{\beta(U_j(y, \tau) - U_j(x, \tau))} \right)^{-1}. \quad (3)$$

For convenience we introduce the temperature as $T = 270/\beta$. (The number 270 is fairly arbitrary and was chosen with the aim to see interesting things at “aesthetic” values of T .) At each time step τ we select N times a particle randomly and move it according to the probability (3). Therefore, each particle may move more than once in one time step and when the number of particles is very high, the probability that it moves k times approaches the Poisson distribution with unit average, $P(k) = 1/(e k!)$. This seemingly minor point plays important role in analytical calculations we shall present later. It is also the source of finite-size effects, briefly discussed at the end of this paper.

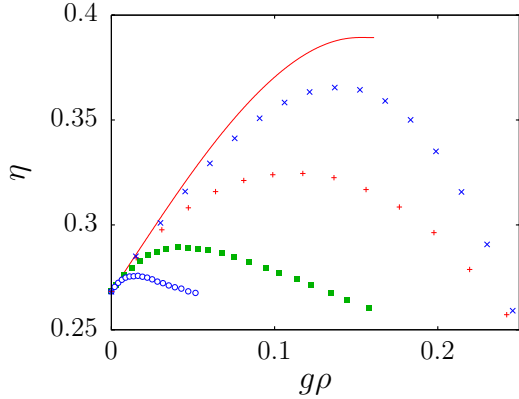


Fig. 4: Dependence of the efficiency on the interaction. To facilitate the comparison of data at various densities with the mean-field approximation, the product $g\rho$ is used as independent variable. We plot the data for four densities, $\rho = 0.1$ (O), 0.3 (■), 1 (+), and 10 (×). The other parameters are $F = 0.1$, $T = 30$, and $t = 16$. The solid line is the result of the mean-field approximation.

The simplest quantity of interest is the current

$$J(\tau) = \sum_i (x_i(\tau + 1) - x_i(\tau)) \quad (4)$$

or rather its time average per particle $J = \lim_{\tau \rightarrow \infty} (\tau N)^{-1} \sum_{\tau'=1}^{\tau} J(\tau')$. The main focus of this work being on the energetics of the motor, we must define the energy input and the useful work done. The latter quantity, at time τ , is $w(\tau) = F J(\tau)$. The energy pumped into the motor from outside relates to the change of the potential $V_a(\tau)$ while the particles stay immobile. Thus, the absorbed energy between steps $\tau - 1$ and τ is

$$a(\tau) = \sum_i (V(x_i(\tau), \tau) - V(x_i(\tau), \tau - 1)) \quad (5)$$

and the efficiency, accordingly,

$$\eta = \frac{\lim_{\tau \rightarrow \infty} \sum_{\tau'=1}^{\tau} w(\tau')}{\lim_{\tau \rightarrow \infty} \sum_{\tau'=1}^{\tau} a(\tau')} \quad (6)$$

The typical results for the current and efficiency can be seen in Fig. 2. Generically, both quantities decrease with increasing temperature. Only for very fast driving i. e. at the smallest values of t , the maxima of current and efficiency occur at non-zero temperatures.

On the other hand, it is the region of larger t that is interesting, as the efficiency grows when t gets longer. At the same time, the current diminishes. This is easy to understand, because slower driving implies lower current but also it leaves the system closer to equilibrium and the loss of energy by non-equilibrium dissipation is therefore also lower. However, as also seen from Fig. 2, for large enough temperature T and force F the trend reverses and η may be even negative. The source of this behaviour is the decrease of the current, not overweighted by decrease

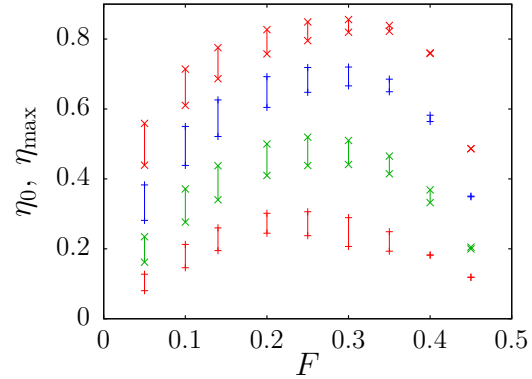


Fig. 5: Comparison of the efficiency at zero interaction η_0 with the maximum efficiency η_{\max} obtained by appropriately tuning the interaction strength g . Each pair of points connected by a vertical line denotes η_0 (lower point) and η_{\max} (upper point). Where only a single point is shown, the maximum is reached at $g = 0$. For all points, we have $L = N = 1200$, $T = 10$. The sets of pairs correspond to quarter-periods $t = 8$ (lower +), 16 (lower ×), 32 (upper +), and 64 (upper ×).

in absorbed energy, when driving gets slower. If a non-zero external force F is applied, the current eventually changes sign and so does also the efficiency.

In Fig. 3a we can see how the efficiency depends on interaction strength. At zero temperature we observe complicated sequence of steps. They are gradually smeared out when temperature increases, until it reaches a function with single maximum, which moves to lower g and eventually disappears when temperature is further increased. This leads to our main observation that within certain interval of temperature (and other parameters), efficiency can be enhanced by the interaction of the motors. However, our simulations show that at the same time the current is suppressed. In Fig 3b we show that the efficiency of the motor at $T = 0$ exhibits complicated dependence on interaction with lots of maxima and the complexity keeps growing when the driving gets slower. Similar complex pattern is seen also for the current.

In Fig. 4 we can see the typical dependence of the efficiency on interaction at a medium temperature. At higher density of particles $\rho = N/L$ the maximum possible increase of efficiency with respect to non-interacting case is higher. This is due to larger role of fluctuations in local particle density, when the number of particles is lower. We can see that the gain in efficiency can be easily larger than 10%, a quite appreciable difference. The dependence of the gain on external force and on the speed of driving is shown in Fig. 5. We can see that the efficiency reaches maximum at certain value of the force and beyond that value the efficiency not only diminishes but eventually becomes non-optimizable by tuning g . i. e. non-interacting case is the most efficient. However, there is quite wide window, where the efficiency can be tuned to optimum by setting both force and interaction to convenient values.

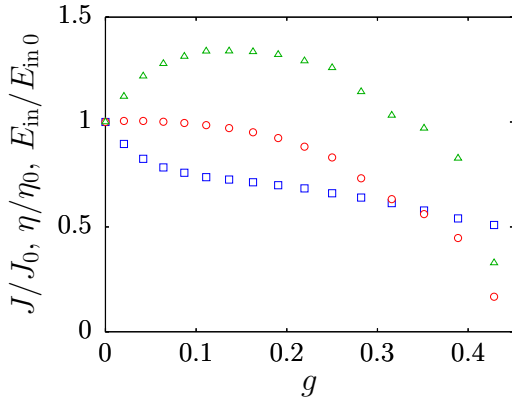


Fig. 6: Current (\circ), efficiency (\triangle) and energy input (\square) relative to their values for $g = 0$. The parameters are $L = N = 1200$, $T = 10$, $t = 16$, and $F = 0.1$.

To gain further insight into the mechanism of efficiency enhancement, we plot in Fig. 6 the dependence of efficiency, work performed and energy input on interaction strength g , all relative to the value for non-interacting ($g = 0$) case. We can see that for small g , the work done is practically interaction-independent and starts to decrease only at larger g . This behaviour copies the dependence of the current, as work is simply current times force. On the other hand, the energy input drops quickly even at small g . This accounts for the net increase of efficiency at small g . For larger g , the decrease in current (i. e. work), outweighs the decrease of input energy and the efficiency drops again. Obviously, both current and efficiency are zero at exactly the same value of g .

The reason why the input energy drops while current stays practically constant when we switch on the interaction can be stated as follows. The particles are essentially driven by the travelling potential wave. At not too high temperature, the depth of the minima of the potential does not influence much the current. Now, weak interaction effectively shifts the potential slightly upwards at the minima, while at the maxima (where particles rarely occur) the potential is unchanged. The depth of the travelling valleys is lowered, but the current carried by them is practically the same. On the other hand, the energy is pumped in by the temporal change of the potential at the position of the particle. The effect of the repulsive interaction is that the particles are less concentrated at the actual potential minimum, but reside with relatively higher probability on the left or right to the minimum. Therefore, the number of particles whose potential energy is increased at a particular moment is lowered in comparison with the non-interacting case. Hence the decrease in the value of the input energy. Note, however, that this explanation is rather sketchy and more subtle effects are also present here.

We complemented the numerical simulations by analytical calculations using the mean-field approximation.

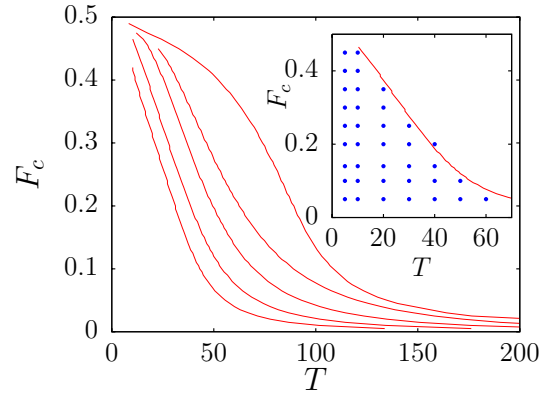


Fig. 7: Phase diagram of the “reversible ratchet”, computed using the mean-field approximation. The lines separate the optimizable (lower-left) phase from the non-optimizable (upper-right) and correspond to quarter-periods $t = 1, 8, 16, 32$, and 64 (from top to bottom). In the inset, the mean-field phase diagram for $t = 32$ accompanied by the results of numerical simulation for $\rho = 0.3$. Each heavy dot in the rectangular grid denotes a pair of variables (T, F) for which maximum efficiency was found at interaction strength $g > 0$.

Although the process representing the movement of the motors is inherently non-stationary and principally non-Markovian, due to periodic external driving, we can describe it equivalently as a Markov process on larger state space and find stationary state for that process. If the particles do not interact, it is enough to study the movement of a single representative particle in the potential (1). The probabilities (3) for one hop of the particle from site x to site y form a time-dependent matrix $W_1(\tau)$. However, as we mentioned, the number of hops the particle actually makes follows the Poisson distribution. The actual transition matrix for the movement of the particle at time τ is therefore $W(\tau) = \sum_{k=0}^{\infty} \frac{1}{k!} (W_1(\tau))^k = \exp(W_1(\tau) - 1)$. Combined positions of the particle at times $\tau, \tau + 1, \dots, \tau + 4t - 1$ evolve according to a Markov process. The only non-zero elements of the corresponding transition matrix W^R are $W_{y\tau+1, x\tau}^R = W_{yx}(\tau)$. While $W(\tau)$ is a time-dependent 3×3 matrix, W^R is a time-independent matrix $12t \times 12t$. If we divide it into 3×3 blocks, we can see that only the blocks below the block diagonal and the single block in the right top corner are non-zero. These non-zero blocks contain the matrices $W(1), W(2), \dots, W(4t)$.

The stationary state p^R of this composite process is the solution of the linear equation

$$p^R = W^R p^R. \quad (7)$$

The average current, work and absorbed energy are then found as linear combinations of the elements of p^R .

The interaction can be taken into account using the mean-field approximation $g n_j(x, \tau) \simeq g \rho p_{x\tau}^R$. Through the hopping probabilities (3) the stationary state p^R penetrates into the matrix W^R and the equation (7) becomes non-linear.

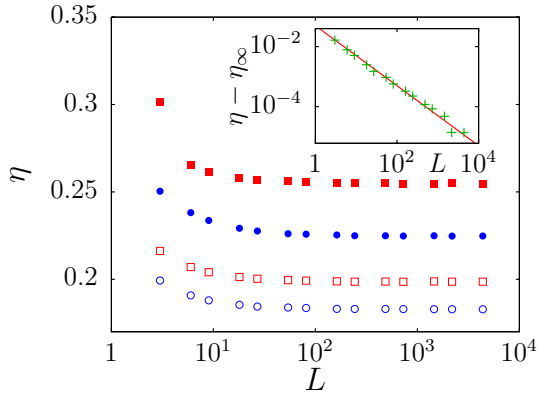


Fig. 8: Effect of finite size on the efficiency, for fixed density $\rho = 1$. Various symbols correspond to $T = 5$ (squares), $T = 30$ (circles), $g = 0$ (empty symbols), $g = 0.1$ (filled symbols). Further parameters are $t = 8$, $F = 0.14$. In the inset, deviation of the efficiency from its asymptotic ($L \rightarrow \infty$) value, for $\rho = 1$, $T = 30$, $t = 8$, $g = 0$ and $F = 0.14$. The line is the power $\propto L^{-1}$.

We can judge from Fig. 4 to what extent the mean-field approximation (MFA) captures the results obtained by numerical simulations. We observe that MFA tends to coincide with simulations when the average density is large, more precisely in the limit $\rho \rightarrow \infty$ with $g\rho$ kept fixed. The reason why MFA works well in the high-density limit (and not in the opposite case $\rho \rightarrow 0$, as one might think) is that MFA is based on neglecting the relative density fluctuations. When the average density is low, changing position of a single particle implies large relative change of local density, while in the high-density regime the change in local density is very small.

It also suggests that the slope of the dependence of η on $g\rho$ for $g\rho \rightarrow 0$ is reproduced exactly in MFA. If the slope is positive, the efficiency can be increased by turning on the interaction. We shall call that optimizable phase. Negative slope means that non-interacting case is the best possible and we shall call that phase non-optimizable. From Fig. 4 we can also see that the sign of the slope does not depend on the density ρ . Therefore, we can draw a phase diagram in the temperature-force plane, like in Fig. 7. The line determines the temperature dependence of the critical force F_c where the slope vanishes. We can see that the area of the optimizable phase shrinks when the driving gets slower (t increases). This is easy to understand, as slower driving itself induces higher efficiency, so there is less room left for further optimization by tuning the interaction strength. In Fig. 7 we also demonstrate that the simulation results for the phase diagram agree reasonably well with the MFA even for relatively low density $\rho = 0.3$, where otherwise the MFA is ill-justified, as seen from Fig. 4.

We also investigated the issue of finite-size effects. In Fig. 8 we show the efficiency for various widths L of the sample, from $L = 3$ to 4374 (recall that L must be a mul-

tipole of 3), with fixed density. We can see that the finite size effects do occur, but can be neglected for sizes larger than about $L \simeq 100$. We can also see that the deviation of the size-dependent efficiency η from its asymptotic value η_∞ for $L \rightarrow \infty$ scales like $\eta - \eta_\infty \sim L^{-1}$. The finite-size effects stem from the probability that a chosen particle makes exactly k moves in one step of the simulation. The distribution converges to Poissonian in the limit $L \rightarrow \infty$, but definitely deviates from it if the number of particles is finite.

To summarise, within the scheme of “reversible ratchet”, we showed that interaction of large number of molecular motors leads to collective effects resulting in substantial increase of energetic efficiency. The price to pay is the decrease of particle current. We also found that the dependence of the efficiency (and current) on interaction strength is very complex at low temperatures, exhibiting complex sequence of multiple maxima and minima. For certain values of the external force it can even become a sequence of current reversals. To check the generic character of our results we performed similar simulations also for the case of rocking ratchet [34]. Also here, we observed increase of efficiency in a window of temperatures and external forces. However, the overall efficiency is order of magnitude lower than in the “reversible ratchet”, thus also the increase is much lower in absolute numbers.

The question to discuss is how we can tune the interaction strength in a real system, where the interaction of motors has actually a hard-core character. In fact, although the motivation of our study was to large extent based on biological experiments, we had in mind possible applications in artificial motors [12] like those of Refs. [10,11], made of micropores. Varying the spatial geometry of the pore we can effectively tune the influence of hard-core repulsion of moving particles. Thus we have another degree of freedom at our disposal in our design of efficient man-made molecular motors.

I gladly acknowledge inspiring discussions with P. Chvosta, E. Ben-Jacob and P. Kalinay. This work was carried out within the project AVOZ10100520 of the Academy of Sciences of the Czech republic and was supported by the Grant Agency of the Czech Republic, grant no. 202/07/0404.

REFERENCES

- [1] M. O. Magnasco, Phys. Rev. Lett. **71**, 1477 (1993).
- [2] M. Schliwa (Ed.), *Molecular Motors* (Wiley-VCH, New York, 2003).
- [3] F. Jülicher, A. Ajdari, and J. Prost, Rev. Mod. Phys. **69**, 1269 (1997).
- [4] P. Reimann and P. Hänggi, Appl. Phys. A **75**, 169 (2002).
- [5] P. Reimann, Phys. Rep. **361**, 57 (2002).
- [6] P. Hänggi, F. Marchesoni, and F. Nori, Ann. Phys. (Leipzig) **14**, 51 (2005).

- [7] R. Lipowsky, Y. Chai, S. Klumpp, S. Liepelt, M. J. I. Müller, *Physica A* **372**, 34 (2006).
- [8] A. B. Kolomeisky and M. E. Fisher, *Annu. Rev. Phys. Chem.* **58**, 675 (2007).
- [9] H. Linke, T. E. Humphrey, A. Löfgren, A. O. Sushkov, R. Newbury, R. P. Taylor, and P. Omling, *Science* **286**, 2314 (1999).
- [10] S. Matthias and F. Müller, *Nature* **424**, 53 (2003).
- [11] C. Kettner, P. Reimann, P. Hänggi, and F. Müller, *Phys. Rev. E* **61**, 312 (2000).
- [12] P. Hänggi and F. Marchesoni, arXiv:0807.1283 (2008).
- [13] R. D. Astumian and M. Bier, *Biophys. J.* **70**, 637 (1996).
- [14] I. Raška, K. Koberna, J. Malínský, H. Fidlerová, and M. Mašata, *Biology of the Cell* **96**, 579 (2004).
- [15] P. De Los Rios, A. Ben-Zvi, O. Slutsky, A. Azem, and P. Golubinoﬀ, *Proc. Natl. Acad. Sci. USA* **103**, 6166 (2006).
- [16] K. Sekimoto, *J. Phys. Soc. Japan* **66**, 1234 (1997).
- [17] H. Kamegawa, T. Hondou, and F. Takagi, *Phys. Rev. Lett.* **80**, 5251 (1998).
- [18] J. M. R. Parrondo and B. J. De Cisneros, *Appl. Phys. A* **75**, 179 (2002).
- [19] H. Qian, *Phys. Rev. E* **69**, 012901 (2004).
- [20] J. M. R. Parrondo, J. M. Planco, J. F. Cao, and R. Brito, *Europhys. Lett.* **43**, 248 (1998).
- [21] T. Schmiedl and U. Seifert, arXiv:0801.3743 (2008).
- [22] J. M. R. Parrondo, *Phys. Rev. E* **57**, 7297 (1998).
- [23] R. D. Astumian and I. Derényi, *Biophys. J.* **77**, 993 (1999).
- [24] F. Jülicher and J. Prost, *Phys. Rev. Lett.* **75**, 2618 (1995).
- [25] P. Reimann, R. Kawai, C. van den Broeck, and P. Hänggi, *Europhys. Lett.* **45**, 545 (1999).
- [26] E. B. Stukalin and A. B. Kolomeisky, *Phys. Rev. E* **73**, 031922 (2006).
- [27] I. Derényi and T. Vicsek, *Phys. Rev. Lett.* **75**, 374 (1995).
- [28] I. Derényi and A. Ajdari, *Phys. Rev. E* **54**, 5 (1996).
- [29] Y. Aghababaie, G. I. Menon, and M. Plischke, *Phys. Rev. E* **59**, 2578 (1999).
- [30] S. Klumpp and R. Lipowsky, *Proc. Natl. Acad. Sci. USA* **102**, 17284 (2005).
- [31] P. Greulich, A. Garai, K. Nishinari, A. Schadschneider, and D. Chowdhury, *Phys. Rev. E* **75**, 041905 (2007).
- [32] A. Basu and D. Chowdhury, *Phys. Rev. E* **75**, 021902 (2007).
- [33] T. Tripathi and D. Chowdhury, *Phys. Rev. E* **77**, 011921 (2008).
- [34] R. Bartussek, P. Hänggi, and J. G. Kissner, *Europhys. Lett.* **28**, 459 (1994).